Key Engineering Materials
ISSN: 1662-9795, Vol. 926, pp 690-699
doi:10.4028/p-y5090o

Submitted: 2021-12-01
Revised: 2022-01-31
Accepted: 2022-02-17
Online: 2022-07-22

Evaluation of Cold Roll Forming Strategies for the Production of a High-Strength Aluminum Hat Profile

Timon Suckow[1,a*] and Peter Groche[1,b]

[1]Institute for Production Engineering and Forming Machines, Technische Universität Darmstadt, Otto-Berndt-Straße 2, 64287 Darmstadt, Germany

[a]suckow@ptu.tu-darmstadt.de; [b]groche@ptu.tu-darmstadt.de

Keywords: roll forming, aluminum, 7075, heat treatment, T6, W-Temper, soft annealing

Abstract. High-strength aluminum alloys, such as the AA7075 alloy, offer great potential for lightweight construction thanks to their high specific strength. However, high strength and low ductility are a challenge for processing these materials. In our study, three different process routes (T6, W-Temper, O) for roll forming of a hat profile are investigated experimentally and in an FE-simulation. Since the targeted production of the hat profile is hindered due to material failure in T6-condition, inline induction heating and subsequent water spray quenching is used to bring the material to the W-Temper state before roll forming. As a third option, a pre heat treatment is applied to a soft annealed (O) material state. The experimental results show fundamental differences of the forming processes, depending on the tempering condition. The FE-simulation involves the roll forming process for the production of a hat profile and shows a high agreement with the experiments. Finally, the experimental results demonstrate how inline solution annealing by induction heating for the W-Temper process affects the properties and the quality of the profiles produced.

Introduction

High-strength aluminum alloys are predestined for lightweight applications [1]. With a tensile strength of at least 540 MPa, AA7075 (T6) is the alloy with the highest strength among commercial aluminum alloys [2]. The AA7075 alloy with its main alloying elements zinc, magnesium and copper is an age-hardenable alloy. This allows a variety of different process routes with adapted heat treatment conditions and process temperatures. The different states are created by varying heat treatments. To produce the high-strength T6-condition, which is usually the as-delivered condition, the material must first be solution annealed at 460 – 480 °C and quenched [1]. The quenching rate must exceed 300 K/s, otherwise strength-reducing precipitates will occur [3]. Quenching is followed by artificial aging at 120 °C for 24 hours. The poor weldability and tendency to stress corrosion cracking are characteristic for the AA7075 alloy [4,5].

The advantageous mechanical properties of the AA7075-T6 alloy cause difficulties in processing, especially for sheet metal forming processes, such as roll forming. Poor formability with cracking at low strains and high springback after forming are the two main challenges [6–8]. The high-strength AA7075 alloy in the T6-condition is not suitable for roll forming of profiles with a small bending radius, such as a hat profile. Roll forming is a stepwise forming process for production of long profiles and allows the integration of additional process operations, e.g. an inline heat treatment or welding operation. For the heat treatable aluminum alloy AA7075, a W-Temper heat treatment [9], and soft annealing [10] lead to a significant increase in formability and thus to an extended process window in metal forming processes.

A variation of the common cold forming process is the W-Temper process, which is named according to the W-condition. The W-condition is obtained directly after solution annealing and quenching [9]. The result of the W-Temper heat treatment is an increased formability for a limited period of time after quenching. Fig. 1 shows the schematic temperature/time-curve for the W-Temper heat treatment of age hardenable aluminum alloys, such as the AA7075 alloy. The forming process is performed during the transition time. After warm aging, the material is in T6-condition again. Another approach to form high-strength aluminum alloys is to soft anneal the material before forming.

For soft annealing, a heat treatment of at least 9 h is suggested by [11], which makes it inappropriate for an inline heat treatment.

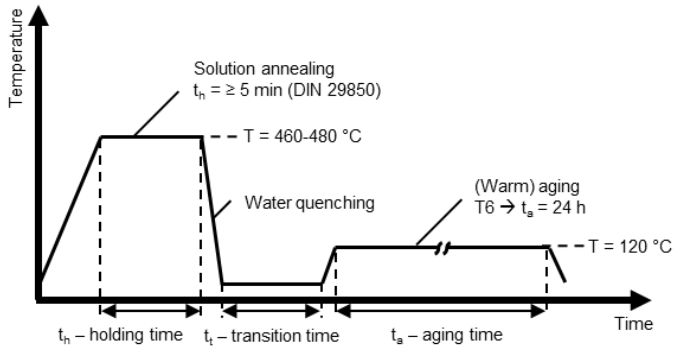

Fig. 1: W-Temper heat treatment with subsequent aging for achieving the T6-condition

FE-Model

The focus in this paper is on the cold roll forming process with three different material conditions (T6, W-Temper and O). Fig. 2 shows an increased formability of the O- and W-condition, compared to T6. Characteristic for the O-condition is the low yield strength $R_{p0,2}$ of 129 MPa and the increased elongation at fracture (A = 12 %), compared to the T6-state. For the W-condition, the elongation at fracture is further increased to A = 21 %, while the yield strength of $R_{p0,2}$ = 163 MPa is higher than in the O-condition. Furthermore, high strain hardening in the W-condition can be noticed. The data were obtained from uniaxial tensile tests according to DIN EN ISO 6892:1 on a tensile testing machine Zwick Roell 100 with a strain rate of 0,002 1/s [12]. The W-Temper specimen were solution annealed at 480 °C and tested three minutes after quenching.

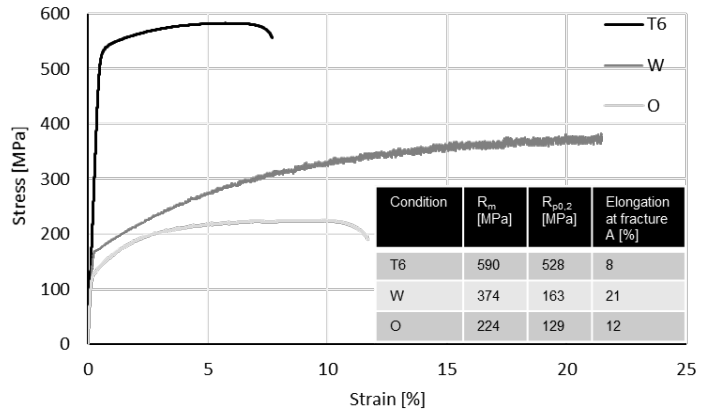

Condition	R_m [MPa]	$R_{p0,2}$ [MPa]	Elongation at fracture A [%]
T6	590	528	8
W	374	163	21
O	224	129	12

Fig. 2: Stress-strain-curves for the AA7075 alloy

The data from the tensile tests are the basis for the flow curves in the FE simulations. The flow curves were approximated using the Ludwik Holomon equation and an isotropic hardening model is applied in the simulations. The elastic behaviour of the material is described by a Young's modulus of E = 72 GPa. For evaluation of the roll forming forces in the simulation, the compliance of the upper rolls is implemented in the simulation by springs, according to former investigations [13,14]. Element type and size are also based on findings from earlier roll forming studies [8,15,16]. Friction is neglected in the FE simulation due to its small influence on the results (geometry and loads) and reduction of computing time [14]. Further boundary conditions, as well as the profile flower for the hat profile are presented in Fig. 3 a and b.

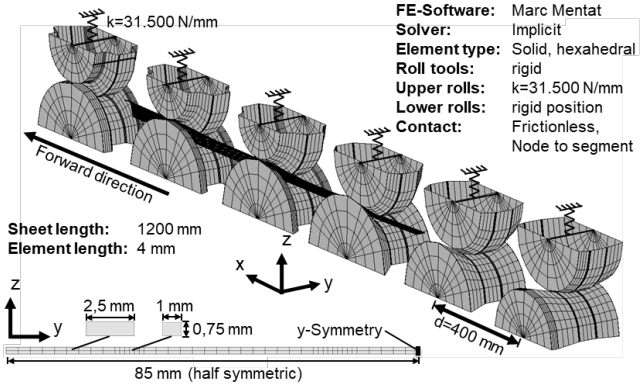

a)

Pass	Inner radius r_1 [mm]	Bending angle α [°]	Inner radius r_2 [mm]	Bending angle β [°]
1	17,00	15	-	-
2	8,05	30	-	-
3	**5,10**	**45**	-	-
4	3,63	60	12,85	30
5	2,90	72	7,35	50
6	3,00	70	5,00	70

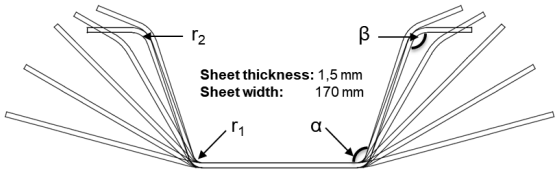

b)

Fig. 3: a) Setup of the FE-model. b) Profile flower for the hat profile

Experimental

The following section describes the experimental setup for the investigations and the methods for evaluation of the results. W-Temper forming requires inline heat treatment, in which the sheet material AA7075-T6 is heated to 460 °C by means of an inductor and then quenched. Fig. 4 a shows the experimental setup for the inline heat treatment. The sheet moves through the inductor (Trumpf MF 5040 HF Generator) with a speed of 1 m/min and is quenched subsequently by water spray. The distance between the inductor and the quenching chamber is 250 mm. A thermocouple and a pyrometer are used for temperature measurement. After quenching, the roll forming process is performed. Ten minutes later, the profiles are artificially aged in a heat treatment furnace for 24 h at 120 °C.

In the process route with the soft annealed (O) material, a 10 h heat treatment is performed. The sheets are heated at 410 °C for 2 hours and then cooled down to 230 °C in a defined manner with a gradient of 30 °C/h. The temperature of 230 °C is kept for 2 h. After air-cooling, the material is in the O-condition and ready for roll forming. The roll forming experiments are performed on a VOEST P 450/4 roll forming machine without lubrication. Fig. 4 b shows the setup for the roll forming experiments. In the roll forming experiments, the sheet length is 2000 mm and the roll gap is set to 1,2 mm, which is 0,3 mm less than the sheet thickness.

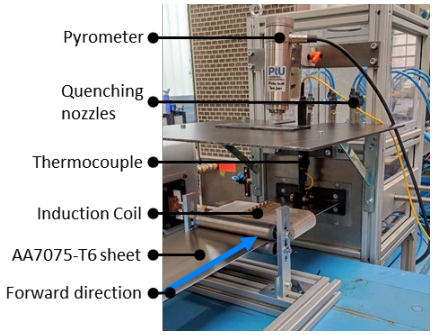

a)

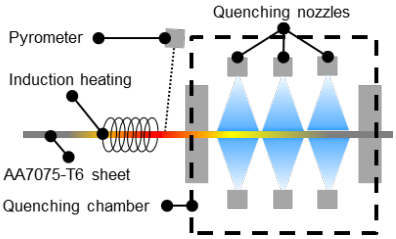

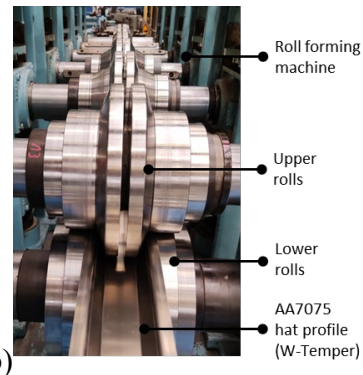

b)

Fig. 4: a) Experimental setup for inline W-Temper heat treatment. b) Experimental setup for the roll forming experiments

Results

Initially, the cold roll forming tests were performed in the T6-condition. Material failure in the form of cracks occurs in the third pass of the process, at a bending radius r_1 of 5,10 mm. Fig. 5 shows the crack initiation in the third pass, directly at the roll contact of the third pass. The experiment results in the demand for an alternative process route.

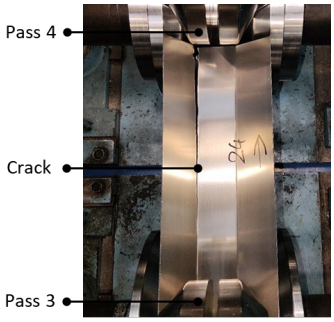

Fig. 5: Crack initiation while roll forming of a hat profile in T6-condition in the third pass

Evaluation of the inline heat treatment. In order to perform the W-Temper experiments, a temperature control for the process is required. Either a pyrometer or a thermocouple can be used for this purpose. The advantage of the thermocouple is the higher accuracy, but the disadvantages are the response time and the temperature stability of thermocouples available on the market. A Fluke Pyrometer E3ML-F0-D-0-0 and a roll-attached thermocouple Type K were used for the experiments. The fact that the thermocouple is approved for temperatures below 450 °C prevents its use in the process. However, the emission coefficient e is determined with the help of the thermocouple. The sheet is heated to a defined temperature under constant speed and thermocouple and pyrometer measurements are compared, as demonstrated in Fig. 6 a. The emission coefficient of e = 0,26 was determined from the tests and applied to the temperature control by a PID controller.

For quality control of the homogeneity of the induction heating, a temperature profile is created with a Fluke TV46-L-0-1 thermographic camera and pyrometer measurements are conducted in the middle and edge areas of the profile. The measurement of the thermographic camera does not claim a high accuracy regarding temperature and is only intended to show the temperature profiles along the sheet width. However, the results of the thermographic camera and the pyrometer are in accordance. As illustrated in Fig. 6 b, the temperature is higher in the band edges, compared to the sheet middle. The error bars of the pyrometer measurement represent the maximum and minimum value of the average of three 30 s measurements. The fact, that the temperature on the left side of the sheet is 25 °C and on the right side 15 °C higher than in the sheet middle makes temperature control more difficult. In accordance with the possible range of the solution annealing temperature from 460 - 480 °C, the temperature in the sheet middle is set to 460 °C in the experiments, to ensure full solution annealing in the sheet and to prevent overheating of the band edge as far as possible. In forward direction, the temperature profile becomes more uniform, thanks to the heat conduction inside the aluminum sheet.

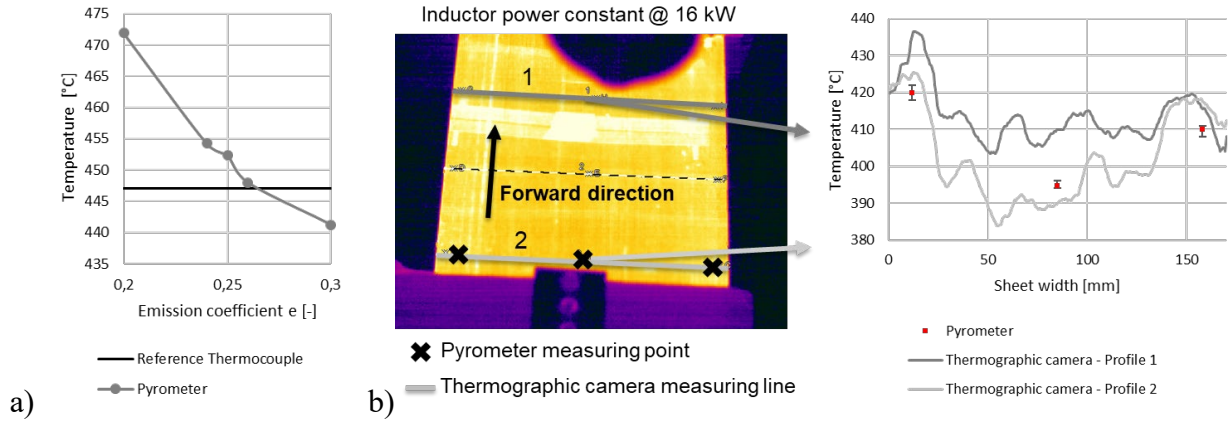

Fig. 6: a) Determination of the emission coefficient for temperature control. b) Temperature distribution after inductive heating

An approach to determine the quality of the inline heat treatment is the hardness measurement after the roll forming process with a comparison of hardness values, determined in reference experiments. For this purpose, idealized heat treatment cycles are performed based on the process conditions of the inline heat treatment. In these experiments, AA7075-T6 sheets are rapidly heated

(approx. 36 K/s) in a contact heating unit and held at the soaking temperature for 10 s before being quenched in water and aged at 120 °C for 24 hours. Subsequently, the hardness measurement on the Struers DuraScan 20 hardness tester follows as a reference for the hardness values in the cross section. Fig. 7 a shows the hardness for different solution annealing temperatures in the range of 420 °C to 500 °C. As expected, the highest hardness values are in the temperature range of 460 - 480 °C, in agreement with the proposed solution annealing temperature in literature. The initial hardness of the T6 base material is 190 HV1, which means an increase of hardness for the short time solution annealing, especially at 480 °C.

For the hardness measurement in the cross section of the profile, the profile is cut after forming and aging and embedded in an epoxy resin matrix. As illustrated in Fig. 7 b, the hardness is high in the band edges with up to 171 HV1, compared to the middle of the sheet, where the minimum hardness is 164 HV1. An additional measurement in the strain-hardened area of the bending radii shows that the values are up to 15 HV1 higher than in the middle of the sheet. This demonstrates that strain hardening from the forming process is retained despite subsequent aging at 120 °C for 24 hours, which is favourable for applications requiring high-strength parts.

The qualitative profile of temperature and hardness measurement is almost the same. Moreover, it is noticeable that the hardness values in Fig. 7 b are smaller compared to the reference tests from Fig. 7 a, especially in the sheet middle. This indicates imperfect in-line heat treatment in the roll forming experiment, primarily resulting from the imperfect temperature distribution in the cross section of the sheet. Additional explanations include the temperature drop from the induction coil to the quenching chamber, as well as the chaotic water quenching process in the quenching chamber. The quenching process is of great importance as the mechanical properties of the AA7075 alloy are sensitive to quenching [3]. For an industrial application of the W-Temper process, the temperature distribution after induction heating must be uniform, and it is recommended to increase the feed rate of the sheet to prevent accidental cooling before quenching. Moreover, the quality of the quenching process can be improved by using an air-water cooling system, to ensure that the minimum recommended quenching speed of 300 K/s is maintained over the whole sheet. However, the quality of the W-condition is sufficient to increase the formability and perform the experiments described in the following section.

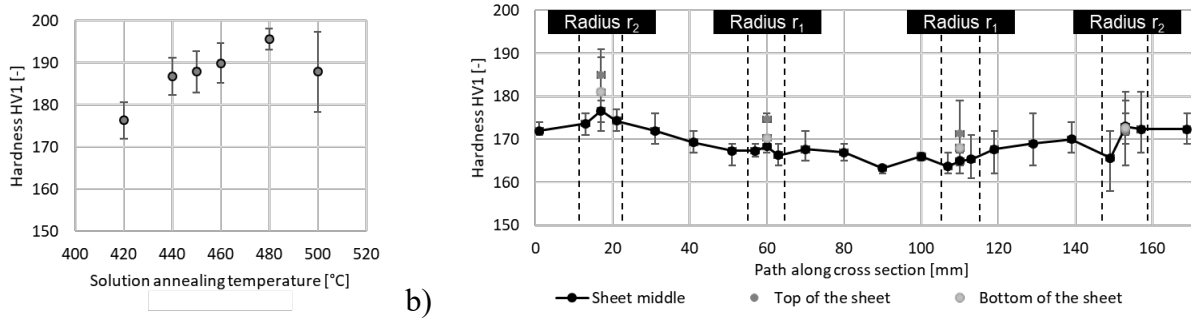

a) b)

Fig. 7: a) Vickers hardness HV1 for different solution annealing temperatures. b) Hardness distribution in the profile after roll forming and aging

Geometry evaluation of the cross section. In the following section, the results of the W-Temper- and O-roll forming experiments are presented. The geometry of the profiles is measured by the GOM ATOS 5 3D scanning system. To determine the experimental results, three profiles are measured for each condition. The error bars represent the minimum and maximum values of springback. Fig. 9 provides an overview of the half-symmetric final geometry of the hat profile after the last forming pass and after springback. The deviation from the nominal bending angle α_1 of 70° is nearly zero for both conditions, especially for the experimentally measured values. Thus, the geometry meets the requirements of DIN EN 10162 [17], so that the process is suitable if typical profile accuracy is required. For the W-condition, the bending angle in the simulation is 2,5 ° higher and for the O-condition 2 °. The prediction of the springback angle by the numerical simulation is thus within a tolerable range.

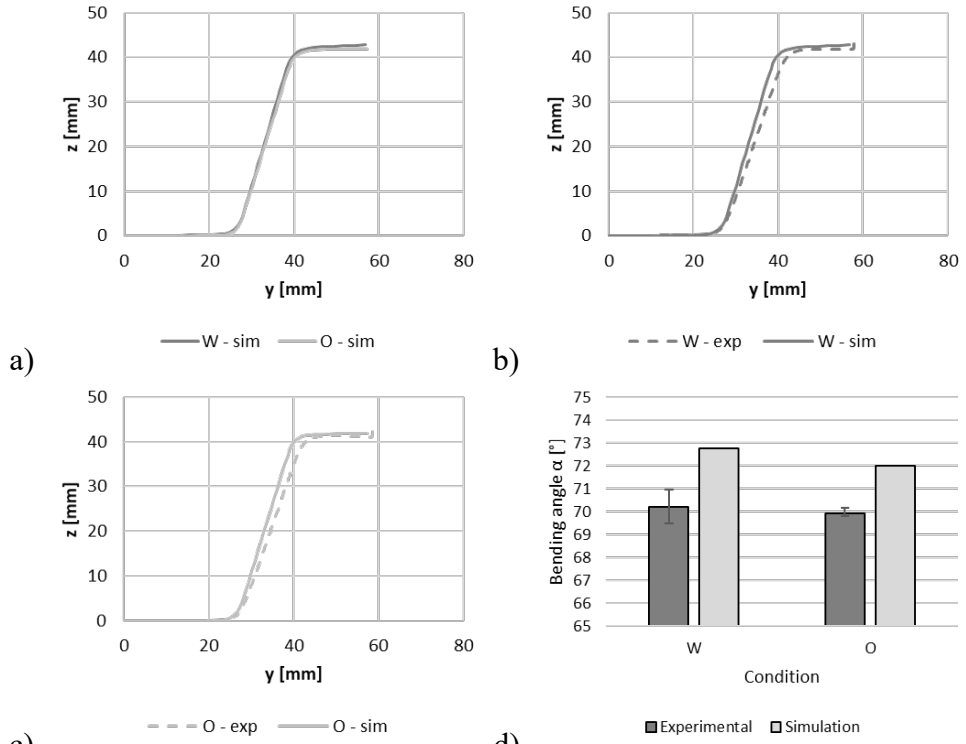

Fig. 8: Geometry of the hat profile after last forming pass and after springback. a) Comparison of the simulation for W- and O-condition. b) Comparison of experiment and simulation for the W-condition. c) Comparison of experiment and simulation for the O-condition. d) Summary of all experiments

Evaluation of longitudinal profile imperfections. Another geometrical parameter for evaluating the profile quality is the longitudinal bow. The bow is measured with the GOM ATOS 5 3D scanning system over a length of 700 mm. In the numerical simulation, the longitudinal bow is calculated in the stationary sheet section from l = 400 mm to l = 800 mm. The occurrence of bow indicates an non-uniform transversal distribution of longitudinal strains in the profile [18]. Fig. 9 a shows the experimental results, compared with the numerical results. The error bars represent the minimum and maximum values of the longitudinal bow. For the O-condition, there is high agreement between simulation and experiment, while the difference is larger for the W-condition. The high value for W-condition could result from a variation of material properties along the profiles cross section due to imperfect heat treatment.

However, the values for the longitudinal bow is still sufficient according to DIN EN 10162 [17], where a maximum value of 2 mm/m is allowed. Fig. 9 b shows a high quality of the geometrical accuracy regarding the path of the band edge in y-direction. No buckling occurs for both, the W- and O-condition in the FE-simulation.

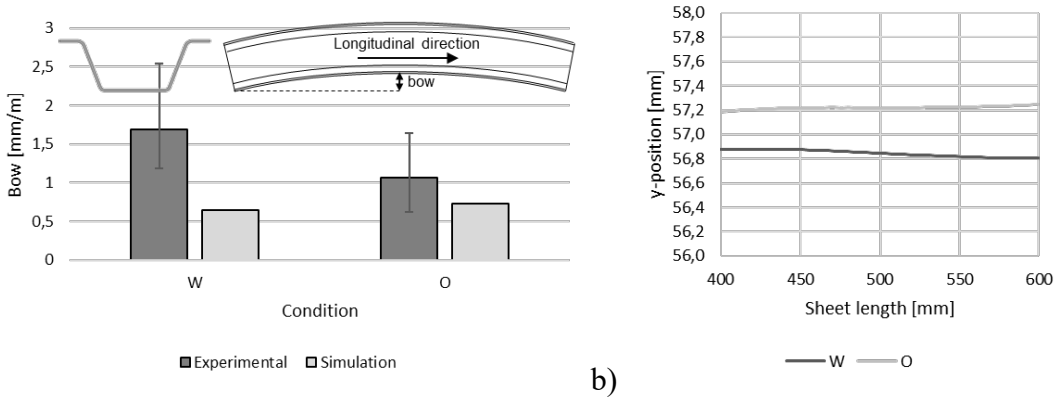

Fig. 9: a) Comparison of longitudinal bow between experiment and simulation. b) Path of the band edge in y-direction in the FE-simulation

Evaluation of roll forming forces. For further validation of the numerical simulation, the force of the upper rolls is measured during the roll forming experiment and compared with the simulation. The force measurement in the tests involves load cells of type HBM C9B, according to the experimental setup in [13]. Fig. 10 shows the comparison between the experimental and numerical results regarding force measurement. According to [19], the experimentally measured force is strongly dependent on the roll gap. However, the measured deviation of the forces is generally small, indicating a high quality of the numerical model. In the first pass, the experimental measured force is higher than the force in the simulation for all conditions, while in the third pass it is the opposite. A good agreement of the force is obtained in the fifth pass. Considering the absolute force values, the force in W-Temper forming increases from pass to pass up to 3500 N in the fifth pass. The soft annealed material requires the lowest forming forces with a maximum of 2500 N in the fifth pass. The high strain hardening in the W-condition leads to a higher increase of forces compared to the O-condition.

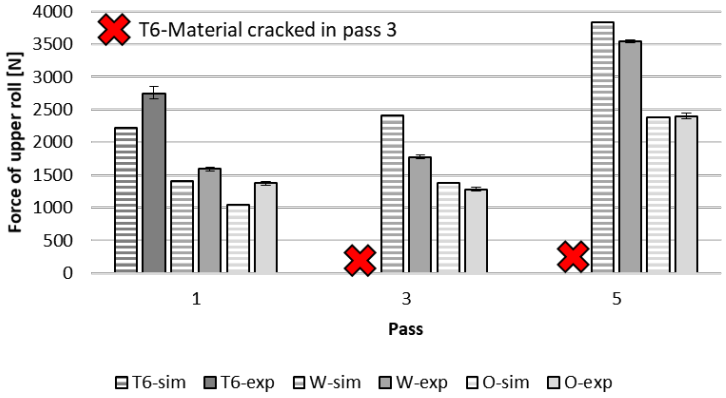

Fig. 10: Experimental and numerical force measurement during roll forming. Average values for the passes 1, 3 and 5

Overall Reflection of the Process Routes

Cold roll forming in the T6-condition is not possible, necessitating alternative process routes. The upcoming W- and O-process routes are compared, based on the experimental results regarding profile quality and an additional energy analysis. As described in the previous chapter, the final geometry is quite close to the desired shape of the hat profile. Springback and longitudinal bow are low and buckling does not occur. In addition, the roll forming process reduces the distortion of the sheet caused by quenching and the requirements of DIN 10162 for cold-rolled profiles are met [17]. The mechanical properties are sufficient for the W-Temper-process and close to the desired T6-condition after forming and aging. Achieving the T6-condition for the soft annealed (O) material requires solution annealing for at least 30 min after forming, followed by quenching and aging.

The assumption for the calculated energy in the energy analysis is the production of a 1000 m hat profile in the desired T6-condition. For this purpose, on the one hand the forming energy and on the other hand the heat energy required for the heat treatment are analyzed and compared. As expected, the plastic forming energy in the W-condition ($E_{forming,\,W}$ = 728 kJ) is higher than in the O-condition ($E_{forming,\,O}$ = 547 kJ), which is due to the higher yield strength and strain hardening. The results are obtained from the FE-model and scaled to the production of 1000 m. Friction losses and efficiency of the roll forming machine are neglected. Fig. 11 provides an overview of the two process chains in terms of quality and energy consumption.

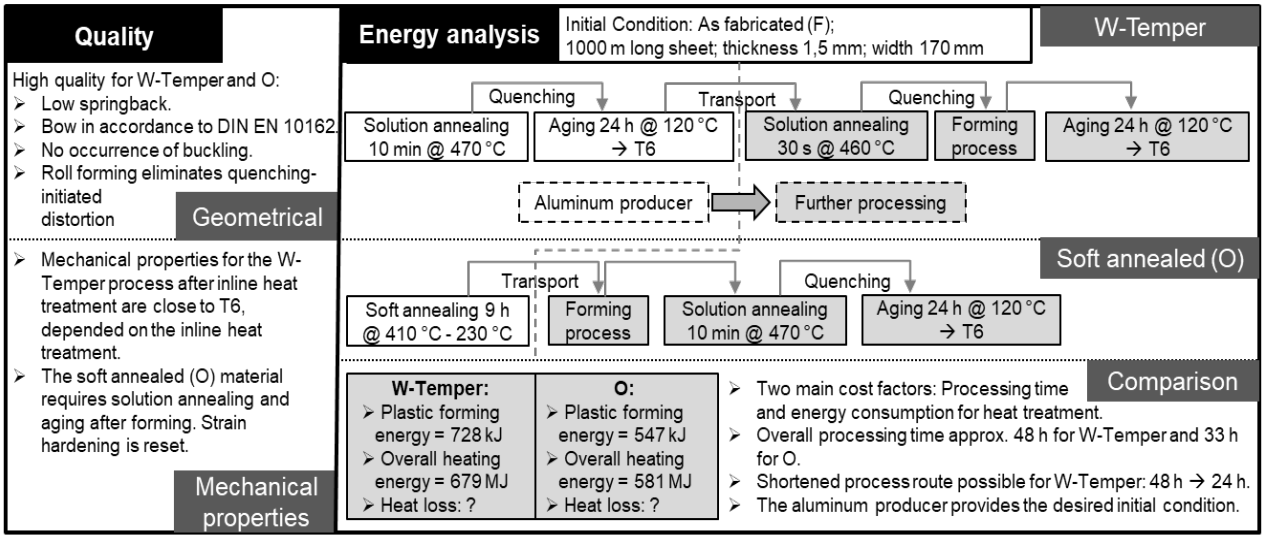

Fig. 11: Overall evaluation of the W-Temper- and O-process routes

The thermal energy analysis serves to present the heating energies as simple as possible and does not claim to be complete due to the high dependence on heating and cooling technology, especially with regard to heat losses and efficiency. The overall heating energy for the W-Temper process is $E_{heating,\,W} = 679$ MJ and for the process with the soft annealed material $E_{heating,\,O} = 581$ MJ, which is remarkably lower. Compared to the forming force, the heating energy is approx. 1000 times higher. For the W-Temper inline heat treatment, the efficiency of the inductive heating was determined to be 25 %, but losses are neglected in the calculation to maintain comparability.

The unknown operating costs and heat losses of the heat treatment furnaces reduce the significance of the calculation, in which only the heating energy is considered. However, the time, effort and energy consumption provide an overview of the process routes. The main cost factors for the process routes from manufacturing side are the time and required temperature for heat treatment. Comparing the total time for the heat treatments of the process routes, the process route for the soft annealed material requires less time for heat treatment compared to the W-Temper process (33 h vs. 48 h).

Since the forming and heating energy as well as the time for heat treatment are higher for the W-Temper process, a higher total energy consumption is also to be expected. However, the W-Temper process allows for a different, more energy-efficient process route, that requires solution annealing and aging are necessary only once. Therefore, the material has to be solution annealed in the F-condition (as fabricated), quenched and directly formed. The time for heat treatments within the process chain is then reduced to 24 h then and the heating energy is reduced to $E_{heating,\,W} = 402$ MJ. This leads to a significant increase in efficiency as well as a reduction in time and costs compared to the process route for the soft annealed material. Considering that heat treatment to achieve the high-strength T6-condition must be performed before or after forming anyway, remarkable process efficiency can be achieved within the W-Temper process. Another advantage of the W-Temper process is the constant furnace temperatures for solution annealing and aging. As described in section 3, soft annealing requires a non-constant temperature profile, which limits the process flexibility for follow up processes.

Summary and Outlook

The investigations in the paper have shown that the material condition has a great influence on the formability of the high-strength AA7075 aluminum alloy. Cold forming of the high-strength AA7075-T6 is not possible, while the W- and O- process routes offer great potential for achieving roll formed profiles with small bending radii. However, the W-Temper process needs to be designed carefully for achieving the maximum profile quality, as demonstrated by the correlation between the heat treatment and the mechanical properties of the final product.

For process design, a complex thermomechanical coupled FE-model is not necessary, since the agreement between mechanical simulation and experiments is sufficient. Finally, the potential for industrial application was shown in the experiments and the energy analysis.

Acknowledgements

The authors gratefully acknowledge financial support from the Hessian State Ministry for Higher Education, Research and the Arts- Initiative for the Development of Scientific and Economic Excellence (LOEWE) for the Project ALLEGRO (Subproject A1).

References

[1] F. Ostermann, *Anwendungstechnologie Aluminium* (Springer-Vieweg Verlag Berlin Heidelberg, 2014).

[2] Deutsches Institut für Normung - DIN, *Aluminium und Aluminiumlegierungen – Bänder, Bleche und Platten*. *Teil 2: Mechanische Eigenschaften* (DIN EN 485-2) (Beuth Verlag GmbH, 2018).

[3] S. Liu, Q. Zhong, Y. Zhang, W. Liu, X. Zhang, and Y. Deng, Investigation of quench sensitivity of high strength Al–Zn–Mg–Cu alloys by time–temperature-properties diagrams, Materials & Design **31**, 3116 (2010).

[4] J. Enz, *Laser beam welding of high-alloyed aluminium-zinc alloys*, Dissertation, Technische Universität, 2017.

[5] S. Russo., P. K. Sharp, R. Dhamari, T. B. Mills, B. R. W. Hinton, G. Clark, and K. Shankar, The influence of the environment and corrosion on the structural integrity of aircraft materials, Fatigue & Fracture of Engineering Materials & Structures **32**, 464 (2009).

[6] B.-A. Behrens, S. Hübner, H. Vogt, O. Golovko, S. Behrens, and F. Nürnberger, Mechanical properties and formability of EN AW-7075 in cold forming processes, IOP Conf. Ser.: Mater. Sci. Eng. **967**, 12017 (2020).

[7] J. Günzel, J. Hauβ, and P. Groche, Temperature-controlled tools for multi-stage sheet metal forming of high-strength aluminium alloys, IOP Conf. Ser.: Mater. Sci. Eng. **1157**, 12086 (2021).

[8] T. Suckow, J. Schroeder, and P. Groche, Roll forming of a high strength AA7075 aluminum tube, Prod. Eng. Res. Devel. **15**, 573 (2021).

[9] E. Sáenz de Argandoña, L. Galdos, R. Ortubay, J. Mendiguren, and X. Agirretxe, Room Temperature Forming of AA7075 Aluminum Alloys, Key Engineering Materials **651-653**, 199 (2015).

[10] B.-A. Behrens, L. Lippold, and J. Knigge, Investigations of the shear behaviour of aluminium alloys, Prod. Eng. Res. Devel. **7**, 319 (2013).

[11] Deutsches Institut für Normung - DIN, *Wärmebehandlung von Aluminium-Knetlegierungen* (DIN 29850) (Beuth Verlag GmbH, 1989).

[12] Deutsches Institut für Normung - DIN, *Metallische Werkstoffe – Zugversuch*. *Teil 1: Prüfverfahren bei Raumtemperatur* (6892) (Beuth Verlag GmbH, 2020).

[13] P. Groche, C. Mueller, T. Traub, and K. Butterweck, Experimental and Numerical Determination of Roll Forming Loads, Steel research international **85**, 112 (2014).

[14] C. Mueller, X. Gu, L. Baeumer, and P. Groche, Influence of Friction on the Loads in a Roll Forming Simulation with Compliant Rolls, Key Engineering Materials **611-612**, 436 (2014).

[15] M. Moneke and P. Groche, Control of residual stresses in roll forming through targeted adaptation of the roll gap, Journal of Materials Processing Technology **294**, 117129 (2021).

[16] M. Moneke and P. Groche, Counter measures to effectively reduce end flare, ESAFORM **2017**, 020006-1 - 020006-6.

[17] Deutsches Institut für Normung - DIN, *Kaltprofile aus Stahl*. *Technische Lieferbedingungen* (DIN EN 10162) (Beuth Verlag GmbH, 2003).

[18] G. Halmos, *Roll Forming Handbook* (Taylor & Francis Group, Boca Raton, 2006).

[19] E. Sáenz de Argandoña, J. Larrañaga, A. Legarda, and L. Galdos, Roll Forming Set-Up Influence in the Forming Forces and Profile Quality, KEM **504-506**, 1249 (2012).